ISBN: 978-3-95450-204-2 ISSN: 2673-5350 doi:10.18429/JACoW-IBIC2019-TUPP020

DEVELOPMENT OF A GATED IPM SYSTEM FOR J-PARC MR

K. Satou†, J-PARC/KEK, Tokai, Japan

Abstract

In the Main Ring (MR) of Japan Proton Accelerator Research Complex (J-PARC), a residual-gas ionization profile monitor (IPM) is used to measure bunched beam profiles. After injection, the beam widths of the first ~20 bunched beams are analysed to correct the Quadruple oscillation. While only a few dozen profiles are required for this correction, the present IPM automatically measures all bunched beams, more than 2E6 bunches from injection to the extraction, because the present IPM operates using DC. This system is undesirable due to the limited lifetime of the Micro Channel Plate (MCP) detector; the more particles the MCP senses, the more it loses gain flatness and thus lifetime. To improve this situation, a gated IPM system has been developed, in which the High Voltage (HV) is operated in pulse mode. Results of performance analysis of a new HV power supply, improvement of the electrodes, and particle-tracking simulation considering the space-charge-electric field of the bunched beam are described.

INTRODUCTION

In the Main Ring (MR) of Japan Proton Accelerator Research Complex (J-PARC), three residual-gas Ionization Profile Monitors (IPMs) have been used: a horizontal type IPM (D2HIPM) and a vertical type IPM (D2VIPM) have been installed in a straight line named Ins_B where the dispersion function is zero; while another horizontal type IPM (D3HIPM) has been installed in the arc section, named Arc_C, where the dispersion function is non-zero. The Twiss parameters at these IPMs are $(\beta_x,\ \beta_y,\ \eta)$ = (12.1 m, 27.3 m, 0 m), (13.1 m, 21.6 m, 0 m), and (8.4 m, 15.5 m, 2.0 m) for D2VIPM, D2HIPM, and D3HIPM, respectively. Details on these IPMs are presented in [1-3].

The IPMs can be operated in ion-collection mode using a strong High Voltage (HV) maximum ±50 kV without a guiding magnetic field (B field). Only D2HIPM has a magnetic system of maximum 0.2 T, and can be operated in electron collection mode with the B field. For all three IPMs, the HV systems and magnetic system are operated under DC.

The chevron-type Micro Channel Plate (MCP) which has 32ch-strip anodes has been used as a particle detector; the width of each anode is 2.5mm. As the MCP is operated in analog mode, the output current distribution across the strips is a one-dimensional beam profile. Because the HV is in DC, the MCP should sense all ionized particles generated by the circulating bunched beams from the injection to the extraction, totalling more than 2E6 bunches. However, the MCP loses its gain flatness the more the charge is multiplied and extracted from the MCP. Moreover, from a practical standpoint, the MCP detector is expensive and cannot be replaced frequently.

The idea of the gated IPM system [4] was developed at the Fermi National Accelerator Laboratory (FNAL) in the USA. In this system, HV gate pulses are used to accelerate the ionized particles onto the MCP detector. By changing the gate width and operational frequency, the operating duty of the IPM can be changed. For example, if it is operated with a duty ratio of 1/100, the lifetime of the MCP detector would become much longer. Moreover, changing the duty ratio can also improve the gain saturation effect [5], because low average output current is preferable for maintaining the gain stability.

To upgrade the existing IPM systems to the gated IPM system, modifications on the electrodes in the chamber were made, and a HV gate generator was developed. In this paper, the details of electrode modifications and the development of the HV gate generator are described.

IMPROVEMENT OF THE ELECTRODES

The electrodes used to generate flat external electric field, thus accelerating the charged particles onto the MCP detector, were improved as follows:

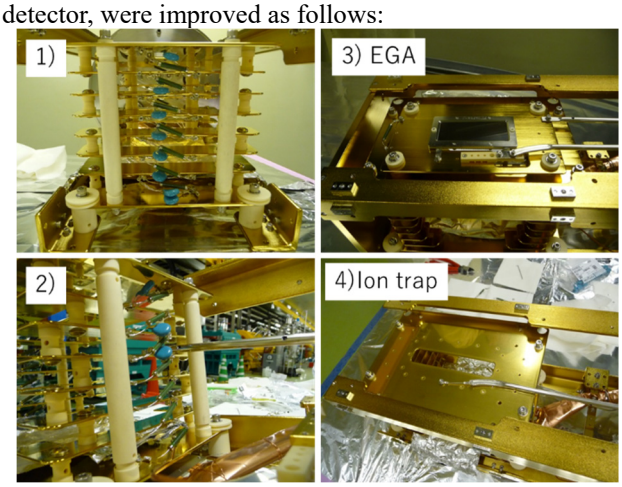

Figure 1: Modifications of the electrodes for gated IPM system. 1), 2)In total 11 capacitors were installed in parallel to the resistors. 3)The Electron Generator Array (EGA) previously installed to check the gain flatness of the MCP detector was removed and 4) an ion-trap structure was newly installed at the same position.

Impedance matching: The rectangular plates at each electrode step, which are used to improve the uniformity of the external electric field, were bridged with a resistor. In this study100 MΩ resistors were used, except for in the last stage where a 50 MΩ resistor was used. To match the impedance and therefore shorten the rise and fall time for the ±30 kV gate pulse signals, 1 nF and 2 nF capacitors were set parallel with the 100 MΩ and 50 MΩ resistors, respectively, as shown as Figs. 1-1 and 1-2.

† kenichirou.satou@j-parc.jp.

ISBN: 978-3-95450-204-2 ISSN: 2673-5350 doi:10.18429/JACoW-IBIC2019-TUPP020

Removal of the EGA: An Electron Generator Array (EGA) plate [6], a large-area electron source, had been previously installed on the top plate of the electrodes as shown in Fig. 1-3. The flat distribution electrons were used to check the gain flatness of the MCP detector. However, the EGA could introduce noise because the ion collisions on its surface generate secondary electrons, and these electrons are accelerated by the external electric fields to the MCP detectors. These signals contaminate with the real signals generated by the ionized electrons. To eliminate the contaminating secondary electrons, the EGA plate was removed.

Ion-trap: After removing the EGA plate, an ion-trap structure was newly installed at the same location, as presented in Fig. 1-4. The operating principle of the ion-trap is reported in [7].

Gain Calibration of the MCP Detector

After removing the EGA, a new beam-based-calibration method was established. To monitor local gain flatness, a bunched beam was shifted transversely in the range of approximately −20 mm to +20 mm by a local bump orbit, and the beam width of the profile measured just after the injection was analyzed. The injected beam width could be measured by the profile monitors in 3-50 beam transport line, and the gain distribution was determined self-consistently. Figure 2 shows the beam profiles before (solid lines) and after (dashed lines) the gain calibration. This demonstrates that the gain in the central area after long-term IPM measurements is only 40% of the initial gain when operations began in 2008.

The estimated beam widths from the calibrated profiles at different positions agreed well, having a standard deviation of 2%. However, a comparison of the beam positions measured by the IPM system and the Beam Position Monitor (BPM) system shows that the beam position from the IPM is smaller than that from the BPM by about 12%. The error sources for this position-mismatch are under investigation.

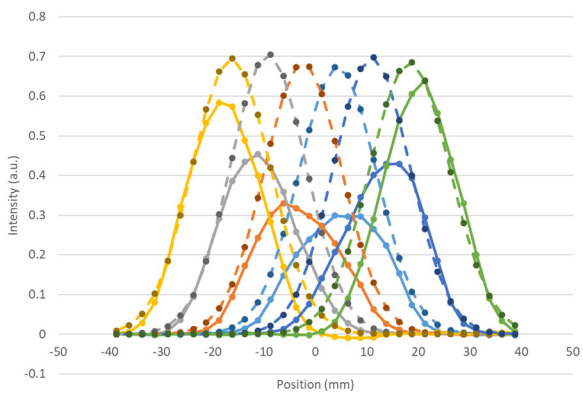

Figure 2: Local gain deterioration of MCP of D2VIPM after long-term operation, since installation in 2008.

Secondary-Electron Suppression by the Ion-Trap Structure

The ion-trap structure can drastically reduce secondary electrons generated by ion collisions from the top plate of the electrodes and the EGA plate. Figure 3 shows how the ion-trap improves the signal purity. These measurements were made using electron collection mode with a guiding magnetic field, where a B field of 0.2 T and HV of −10 kV was applied, and the bias voltage set for the MCP detector was 1.9 kV for both cases. In this experiment, the HV was in DC because the new HV gate generator has not yet been installed. As shown in Fig. 3-1, the contaminated signals appeared in the side areas of the MCP detector. With the use of the ion-trap, almost all the contaminated signals disappeared, and the total signal intensity was reduced to 1/10. The signal intensity level was similar to that obtained using ion-collection mode. These results suggest that almost all the contaminated electrons originated from the ion bombardments on the top plate and the EGA, and could be suppressed by the ion-trap structure.

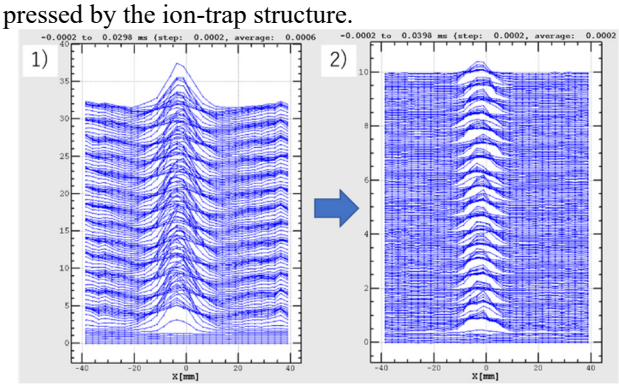

Figure 3: Profiles obtained by electron collection mode using 0.2 T B field and -10 kV collection HV applied on the top plate: 1) from the original IPM design with the EGA on the top plate and 2) from the new design with the ion-trap structure.

30KV GATE GENERATOR

Figure 4 shows a photo of the interior of the 30kV gate generator unit. In this unit, there are three DC HV Power Supplies (PSs): +30 kV DC (1 mA), −30 kV DC (1 mA), and ±20 kV DC (0.6 mA), a 30 kV-30 A MOSFET Push-Pull switch (rise and fall time: ~20 ns), and 35 kV relay switches which are used to pull out charge stored in the system when the HV polarity is changed.

ISBN: 978-3-95450-204-2 ISSN: 2673-5350 doi:10.18429/JACoW-IBIC2019-TUPP020

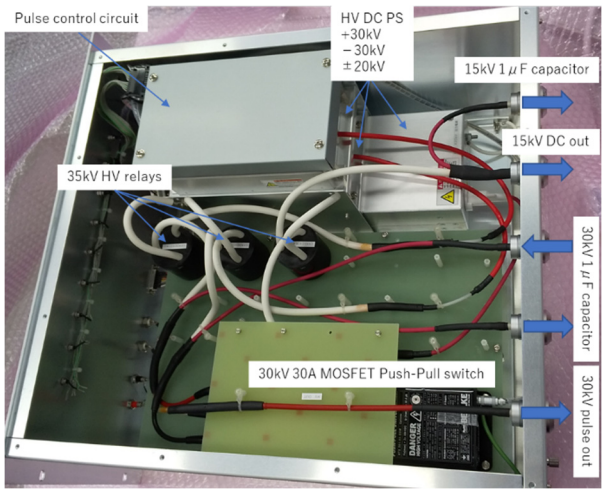

Figure 4: Photo of the ±30 kV gate generator interior.

A simplified block diagram of the 30 kV gate generator is shown in Fig. 5. When the MOSFET switch is turned on, a part of the charge stored in the charge reservoir moves into the coaxial cable. The impedance of the IPM electrodes seen by the cable does not match the 50 Ω characteristic impedance of the HV coaxial cable; the cable can be represented as a simple capacitor of 6.6 nF in total. On the other hand, the impedances between each stage of electrodes are matched except for in the last stage, so the rise time of the HV gate pulse is practically determined by the output current intensity through the MOSFET switch. The voltage applied on the top plate of the electrodes is thus the voltage of the charge reservoir.

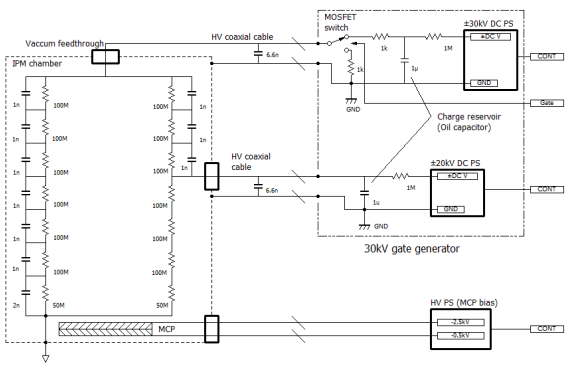

Figure 5: Block diagram of the HV switching system.

Rise and Fall Time of the HV Gate Pulse

The switching performance of the gate generator was checked using a dummy load that simulates a similar impedance to that of the electrodes in the IPM chamber, using HV coaxial cables with a 13 nF total capacitance. The 10%-to-90 % rise (fall) time was 28 μs and the SPICE model was able to closely reproduce the pulse shape. The time would be reduced to 14 μs if the actual HV cable, with a 6.6 nF total capacitance, were used.

Maximum Operation Cycle

The voltage drop when the MOSFET switch is operated is recovered by an output current from the HV DC PSs. Therefore, the stability of the voltage at the electrodes is determined by the current, repetition frequency, and turn on time. The maximum cycle of operation is thus determined to be 10 Hz, with a turn-on time of 100 μs. Such operation would reduce HV at the IPM electrodes by approximately 10%.

SIMULATIONS

Electron motions in the IPM chamber while the gate is off were simulated using a 3D particle-tracking code for IPM design, IPMsim3D [8, 9], where the assumed parameters were a beam size of σt=10 ns, σx=2.7 mm, σy=4.4 mm, and a beam intensity of 4E13 particle per bunch. The peak potential and electric field were therefore estimated to be 47 kV and 2 MV/m, respectively. When the external electric field (Ec) is off, the motions are governed by the space charge electric field (Es) and the guiding magnetic field. Strong horizontal Ec and vertical B causes the E×B to drift along the beam axis, as shown in Fig. 6, as it rotates around the B field. The electrons finally gain vertical momentum, accelerated by the vertical Es of the bunched beams. Figure 6 also shows the Total Kinetic Energy (TKE) distribution of electrons that passes the bottom plane of electrodes. Because the surface of the MCP has a bias voltage of −2.5 kV, only a small fraction, less than 1.2% of the ionized electrons with a TKE larger than 2.5 keV, could reach the surface of the MCP detector.

ISBN: 978-3-95450-204-2 ISSN: 2673-5350 doi:10.18429/JACoW-IBIC2019-TUPP020

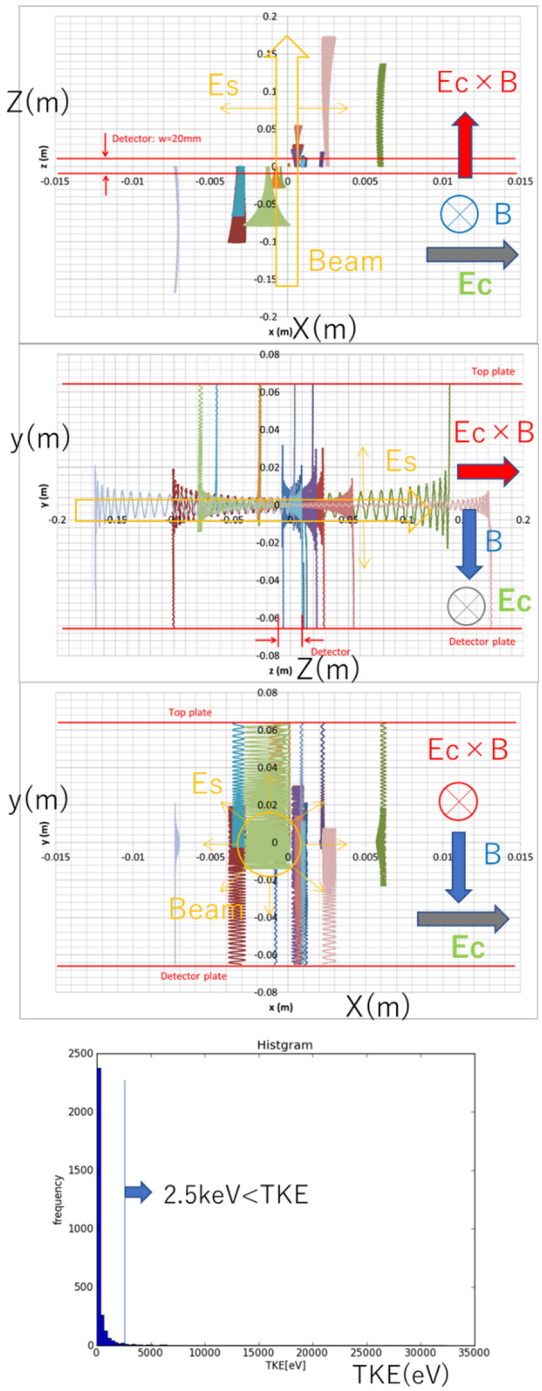

Figure 6: Examples of simulated electron motions in the gated IPM during the gate-off state, in the presence of beam space charge electric field (Es), external electric field (Ec) generated by the electrodes, and magnetic guiding field (B).

INSTALLATION OF THE 30KV GATE GE-GENNERATOR

The new gate generator will be used for the D2HIPM and D2VIPM devices connected in parallel. The installation will be made this autumn, and the first beam operation will start this winter. The first results will be presented at a forthcoming conference.

ACKNOWLEDGEMENTS

This work has been financially supported by the scientific program, Accelerator and Beamline Research and Technology Development for High-Power Neutrino Beams in the U.S.-Japan Science and Technology Cooperation Program in High Energy Physics. The author would like to express deepest thanks to Mr. J.R. Zagel and Dr. R. Thurman-Keup of FNAL for their friendly supports on the HV gate generator development and many informative discussions on the gated IPM system.

REFERENCES

[1] K. Satou, H. Harada, N. Hayashi, S. Lee, T. Toyama, and A. Ueno, "IPM Systems for J-PARC RCS and MR", in Proc. 46th ICFA Advanced Beam Dynamics Workshop on High-Intensity and High-Brightness Hadron Beams (HB'10), Morschach, Switzerland, Sep.-Oct. 2010, paper WEO1C05, pp. 506-510.

[2] K. Satou et al., "Beam Diagnostic System of the Main Ring Synchrotron of J-PARC", in Proc. 42nd ICFA Advanced Beam Dynamics Workshop on High-Intensity and High-Brightness Hadron Beams (HB'08), Nashville, TN, USA, Aug. 2008, paper WGF11, pp. 472-474.

[3] K. Satou, H. Kuboki, and T. Toyama, "Profile Measurement by the Ionization Profile Monitor with 0.2T Magnet System in J-PARC MR", in Proc. 5th Int. Beam Instrumentation Conf. (IBIC'16), Barcelona, Spain, Sep. 2016, pp. 811-814. doi:10.18429/JACoW-IBIC2016-WEPG69

[4] J. R. Zagel *et al.*, "Third Generation Residual Gas Ionization Profile Monitors at Fermilab.", in *Proc. 3rd Int. Beam Instrumentation Conf. (IBIC'14)*, Monterey, CA, USA, Sep. 2014, paper TUPD04, pp. 408-411.

[5] L. Giudicotti, "Time dependent model of gain saturation in microchannel plates and channel electron multipliers", Nucl. Instr. And Meth. A 659 (2011) pp 336-347.

[6] https://www.photonis.com/products/electron-generator-arrays

[7] K. Satou, J.W. Story, S. Levasseur, G. Schneider, D. Bodart, M. Sapinski, "A novel field cage design for the CPS IPM and systematic errors in beam size and emittance", Journal of Physics: Conf. Series 1067 (2018) 072008.

[8] https://twiki.cern.ch/twiki/bin/view/IPMSim

[9] M. Sapinski et al., "Ionization Profile Monitor Simulations - Status and Future Plans", in Proc. 5th Int. Beam Instrumentation Conf. (IBIC'16), Barcelona, Spain, Sep. 2016, pp. 520-523. doi:10.18429/JACoW-IBIC2016-TUPG71